Testing Ion Exchange Resin for quantifying bulk and throughfall deposition of macro and micro-elements on forests

Marleen A.E. Vos[1a], Wim de Vries[2], G.F. (Ciska) Veen[3], Marcel R. Hoosbeek[4], Frank. J. Sterck[1]

[1]Forest Ecology and Forest Management Group, Wageningen University and Research, Wageningen 6700AA, the Netherlands
[2]Earth Systems and Global Change Group, Wageningen University and Research, Wageningen 6700AA, the Netherlands
[3]Department of Terrestrial Ecology, Netherlands Institute of Ecology (NIOO- KNAW), Wageningen 6700AB, The Netherlands
[4]Soil Chemistry Group, Wageningen University and Research, Wageningen 6700AA, The Netherlands

Correspondence to: Marleen A.E. Vos (marleen.vos@wur.nl)

Abstract. Atmospheric deposition is a major nutrient influx in ecosystems while high anthropogenic deposition may disrupt ecosystem functioning. Quantification of the deposition flux is required to understand the impact of such anthropogenic pollution. However, current methods to measure nutrient deposition are costly, labor intensive and potentially inaccurate.

Ion Exchange Resin (IER) appears a promising cost- and labor-effective method. The IER-method is potentially suited for deposition measurements on coarse time scales and for areas with little rainfall and/or low elemental concentrations. The accuracy of the IER-method is, however, hardly classified beyond nitrogen. We tested the IER-method for bulk deposition and throughfall measurements of macro and micro-elements, assessing resin adsorption capacity, recovery efficiency, and field behavior.

We show that IER is able to adsorb 100% of Ca, Cu, Fe, K, Mg, Mn, P, S, Zn and NO_3^- and >96% of P and Na. Loading the resin beyond its capacity resulted mainly in losses of Na, P, NH_4^+ while losses of Ca, Cu, Fe, Mg, Mn and Zn were hardly detected. Heat (40°C), drought and frost (-15°C) reduced the adsorption of P by 25%. Recovery was close to 100% for NH_4^+ and NO_3^- using KCl solution (1 or 2M) while high (83-93%) recoveries of Ca, Cu, Fe, K, Mg, Mn and S were found using HCl as an extractant (2-4M). We found good agreement between the conventional and the IER-method for field conditions.

Overall, IER is a powerful tool for the measurement of atmospheric deposition of a broad range of elements as the measurements showed high accuracy. The IER-method has therefore the potential to expand current monitoring networks and increase the number of sampling sites.

1   Introduction

Atmospheric deposition is a major nutrient influx in many ecosystems and therefore crucial for ecosystem functioning (Van Langenhove et al., 2020). However, due to anthropogenic pollution, atmospheric deposition can potentially disrupt ecosystem nutrient balances, leading to exceedance of critical deposition thresholds of for example nitrogen which can in turn degrade ecosystem functioning (Rabalais, 2002; de Vries et al., 2011). Such degradation of ecosystems involves accelerated soil acidification and reduced availability of critical soil nutrients, such as base cations, which has detrimental impacts on biodiversity and water quality (Houdijk et al., 1993; Johansson et al., 2001; Stevens et al., 2004; Bowman et al., 2008; Horswill et al., 2008; Solberg et al., 2009; de Vries et al., 2014; Lu et al., 2014). Atmospheric deposition is therefore of major importance to many ecosystems and monitoring deposition is necessary for policy, management, and conservation.

Measurements of atmospheric deposition are, however, costly and labor intensive. Direct measurements of dry deposition (i.e. input of elements as airborne particles) and wet-only deposition (i.e. input of elements via precipitation) (Lovett and Reiners, 1986; Balestrini et al., 2007) are scarce and current technology limits widespread measurements. For forests, the common method to assess total deposition (i.e., wet and dry deposition combined) is the collection of precipitation below forests, called throughfall, in collection devices of various shapes and sizes, while accounting for canopy exchange (Draaijers et al., 1996; Thimonier, 1998), which is based on the additional measurement of precipitation outside the forest, known as bulk deposition. The combined measurement of nutrient inputs in precipitation in and outside forests, further called in this paper the bulk deposition method, is readopted in many monitoring networks (i.e. ICP forest network (Bleeker et al., 2003; de Vries et al., 2003; De Vries et al., 2007), the DONAIRE network (Pey et al., 2020) and the nationwide monitoring network in China (Xu et al., 2019)). However, the use of bulk deposition measurements requires frequent (up to weekly) sampling as ammonium in the collected rainwater may relative rapidly be transformed to nitrate by nitrification, with the speed being dependent on local weather conditions (Nicholas Clarke and König, 2016). The high sampling frequency and the high cost of traveling and laboratory analysis, limits the spatial and temporal scales at which this method can be applied. The alternative is larger sampling intervals, but this may cause inaccurate assessment of the input, especially of ammonium versus nitrate. An adequate assessment of both N compounds is especially crucial in regions where the allocation of N sources is highly sensitive (ammonium being caused by NH_3 emissions from agriculture and nitrate from NO_x emissions by traffic and industry). Better alternatives are needed to measure deposition efficiently in the field, improve the reliability of the measurements, reduce sampling effort and costs, and thus allow for more effective large-scale deposition monitoring programs.

The Ion Exchange Resin method (IER) was previously developed to measure bulk deposition at large spatial and temporal scales, but use of the method is yet limited to remote areas (Brumbaugh et al., 2016) the monitoring network of California (Fenn et al., 2018) or case studies (Clow et al., 2015; Garcia-Gomez et al., 2016; Hoffman et al., 2019). Wide-spread application of the IER-method is promising as the method allows to measure the accumulated deposition over long time periods (up to a year), which strongly reduces both the sampling effort in the field and the number of lab analysis, leading to major

60   cost savings (Fenn and Poth, 2004; Kohler et al., 2012). Furthermore, the method is more reliable for nitrogen, as the resin likely inhibits mineralization, nitrification, and denitrification, which can be affected by local weather conditions, as discussed by Fenn and Poth (2004) and Kohler et al. (2012). Finally, the IER-method is able to measure the deposition in areas with low rainfall or low elemental concentrations, avoiding problems with detection limit and minimal sample size required in the bulk deposition method (Kohler et al., 2012).

65   The IER-method is most commonly used for NH_4^+ and NO_3^- measurements (Fenn et al., 2002; Fenn and Poth, 2004; Fang et al., 2011; Kohler et al., 2012; Clow et al., 2015; Garcia-Gomez et al., 2016; Hoffman et al., 2019), but few studies reported measurements of other elements (e.g. S, K, Ca, Mg, Na and Cl) (Van Dam et al., 1987; Simkin et al., 2004; Fenn et al., 2018). The applicability of the method to measure a broad range of elements depends on the performance of the resin, measured as the adsorption capacity (percentage of the total element flux bound to the resin) and the recovery efficiency of elements

70   (percentage of the total element flux recovered from the resin) (Garcia-Gomez et al., 2016). Often though the adsorption capacity and recovery efficiencies are not reported (Fenn and Poth, 2004; Boutin et al., 2015; Fenn et al., 2015; Risch et al., 2020). Studies reporting the adsorption capacity (Simkin et al., 2004; Fang et al., 2011; Garcia-Gomez et al., 2016) describe only the adsorption of a limited number of elements under laboratory conditions. Recovery efficiency under laboratory conditions is more often reported, with in general high recovery efficiencies (87-100%) although the recovery of some macro

75   elements (i.e. Ca and Mg) was below 50% (Simkin et al., 2004; Fang et al., 2011; Kohler et al., 2012; Clow et al., 2015; Wieder et al., 2016; Cerón et al., 2017). Despite the promising applicability, the adequacy of the IER-method to derive bulk deposition and throughfall under field conditions is hardly tested. The limited information on adsorption capacity combined with bad recoveries for some elements (i.e., Ca, Mg, Fe and Al) potentially limits the use of the IER-method for bulk deposition measurements.

80   The adsorption capacity and the recovery efficiency can be influenced by environmental field conditions like drought, frost or high temperatures (Qian and Schoenau, 2002; Bayar et al., 2012). However, there is hardly any study testing the influence of environmental field conditions on both the adsorption capacity and the recovery efficiency of the resin. Furthermore, most tests refer to bulk deposition, whereas atmospheric deposition on forest is also measured as throughfall underneath vegetation canopies. Dissolved organic substances are higher in throughfall than in bulk deposition for which the adsorption capacity of

85   the resin is lower (Langlois et al., 2003). Overall, recovery rates from resin exposed to environmental field conditions appear to be lower, urging the need for better evaluation of IER performance under field conditions (Krupa and Legge, 2000; Brumbaugh et al., 2016). Therefore, new tests are necessary to evaluate the effect of environmental conditions and organically-rich throughfall on the elemental recovery from the resin.

The recovery efficiency can be optimized by the use of different extraction methods. An often used extraction method is 2M

90   KCl for nitrogen extraction (Fenn et al., 2002; Garcia-Gomez et al., 2016; Hoffman et al., 2019), but also combinations of either KI, HNO_3, NaCl, H_2SO_4 and HCl were used (Van Dam et al., 1991; Kohler et al., 2012; Brumbaugh et al., 2016; Fenn

et al., 2018). The KCl extraction method and the KI extraction method do not allow measurements of K deposition and are, as high dissolved salt solutions, problematic for measurements using inductively coupled plasma-atomic emission spectrometers (ICP-AES) (Hislop and Hornbeck, 2002; Brumbaugh et al., 2016). New tests are therefore needed to increase the recovery efficiency allowing to measure a broad range of elements including all macronutrients and micronutrients.

In this study we aim to test the capacity of IER as a method to quantify atmospheric deposition for a broad range of macro- and micro-elements, comparing results under laboratory and field conditions and in the latter case comparing bulk deposition and throughfall. We first tested the method under controlled laboratory conditions to indicate efficient resin volumes and to assess adsorption capacities and recovery efficiencies. Next, the behavior of the IER-method was tested under field conditions covering a gradient from closed forests to open areas to account for the effect of dissolved organic substances on the performance of the resin columns. From this, we provide different methodological protocols with accuracies for detecting different macro- and micro elements under field conditions, including forests.

2   Methods

2.1   Preparation of the resin columns

We prepared 45 resin columns for the laboratory tests of elemental adsorption and recovery (including the blanks), followed by the preparation of 30 columns for the field test of the IER-method. The resin columns had a volume of 15.7ml and an inner diameter and length of respectively 12.4 and 130mm. First, the empty resin columns were cleaned using 0.2M HCl and demineralized water to remove weakly attached chemicals from the column walls. Then, the cleaned and dried resin columns were washed three times with demineralized water in the laboratory prior to filling the column with IER to ensure the removal of any remaining HCl. To fill the columns, a plug of clean polyester fiber was placed inside the resin column and pushed to the bottom. A cleaned cap was screwed loosely at the bottom of the resin column, stabilizing the polyester plug. The resin column was placed vertically above a container to collect the reagents. The ion exchange resin (Amberlite IRN 150, a 1:1 mixture of H^+ and OH^-) was washed with 8L demineralized water in batches of 500g of resin to remove small particles within the resin and to remove the resins smell which could attract animals. All liquids were drained from the resin using a vacuum pump, and for each resin column 9.8g of resin was weighed out and poured in the resin column using a pipette with demineralized water. When excess water had passed through, a second plug of polyester fiber was placed on top of the resin and both sides of the column were screwed tightly with cleaned caps. A schematic overview of these steps is in figure 1.
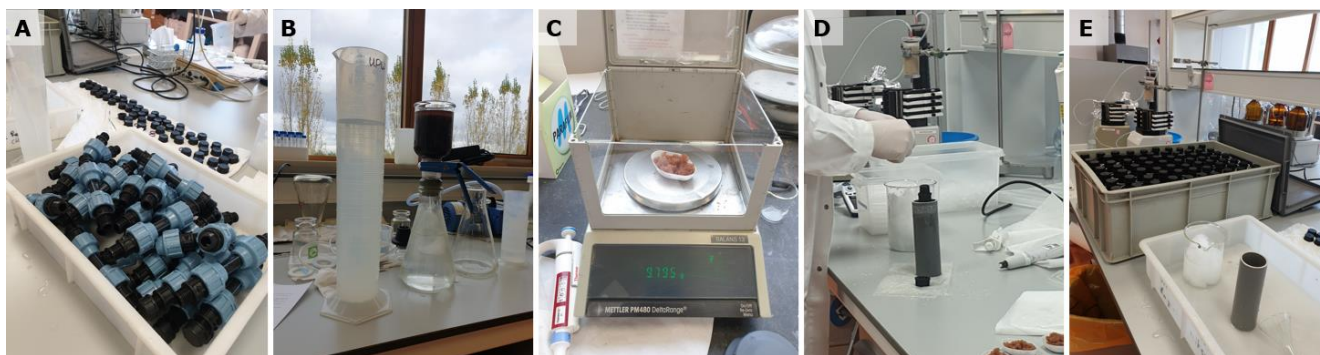
Figure 1: Preparation of the resin columns. A: Cleaned resin columns prior to filling with IER. B: cleaning of the Amberlite IRN-150 exchange resin using a vacuum pump. C: Weighing the resin prior to filling the resin column. D: Resin column stabilized in a holder during filling with resin. E: Overview of filled resin columns with the resin column stabilizer and the polyester plugs shown in the front.

2.2   Laboratory tests

The adsorption capacity and recovery efficiency of the IER (Amberlite IRN 150 H$^+$ and OH$^-$ form) was tested at the Soil Chemistry Laboratory (CBLB), Wageningen University. First, based on existing wet-deposition data from nearby measurement stations located in Biest Houtakker, Speuld, De Zilk and Vredepeel (NL) (RIVM, 2015), we estimated the bulk deposition amounts (kg ha^{-1}) for different elements, and then used those to determine the needed molarity of the solution that was used to test the adsorption capacity of the resin. Both the adsorption capacity and recovery efficiency were subsequently tested for annual maximum bulk deposition rates across the Netherlands of the following elements: PO$_4^{2-}$, SO$_4^{2-}$, N-NO$_2^-$ + N-NO$_3^-$, N-NH$_4^+$, Ca^{2+}, Mg^{2+}, K$^+$, Na$^+$, Fe^{2+}, Mn$^{2+,}$ Cu^{2+} and Zn^{2+}.

To estimate the maximum bulk deposition values, the monthly measurements of existing bulk deposition data of the nearby weather stations (umol l^{-1}) (RIVM, 2015), were summed to seasonal concentrations, expressed in mg L^{-1}. Then, the stations were selected with the highest seasonal deposition, occurring during summer, for both macro- and micronutrients, based on the total molarity of the rainwater. These seasonal concentrations were then multiplied by the precipitation (in L) that would be captured by the funnel, by multiplying the recorded precipitation (in mm or L m^{-2}) with the horizontal surface of the funnel (in m^2) to estimate the total deposition captured by a funnel. Then, the deposition of the summer was multiplied by 2, which is an average multiplication factor to convert bulk deposition to throughfall. This average multiplication factor is based on the reported values for the ratio throughfall/bulk deposition of the tracer Na (Table S1). The total elemental content of this throughfall flux, multiplied by 4 (assuming that the summer values are representative of the entire year, which is a precautionary approach), was dissolved in a 1 L solution separately for macro and micronutrients using stock solutions resulting in an extraction solution containing values reflecting the maximum annual total deposition in the Netherlands (Table 1).

145

Table 1: The throughfall flux used to test the adsorption capacity and recovery efficiency of the ion exchange resin. We used stock solutions with known molarity to make the macro and the micro solution used to drip through the resin. The total volume of the used stock solution (in ml L^{-1}) and the concentration in umol per element are given.

Stock solution Code	Mol	Type	Total mL L^{-1}	Ca	Cu	Cl	Fe	K	Mg	Mn	Na	PO$_4$	SO$_4$	Zn	NH$_4^+$	NO$_3^-$
									umol							
Na$_2$SO$_4$	0.5	Macro	0.90								450		450			
NaCl	1	Macro	1.40			1400					1400					
KNO$_3$	1	Macro	0.18					180								180
KH$_2$PO$_4$	1	Macro	0.02					20				20				
NH$_4$NO$_3$	1	Macro	1.82												1820	1820
NH$_4$Cl	1	Macro	2.18			2180									2180	
MgSO$_4$	1	Macro	0.3						300				300			
CaCl$_2$	0.5	Macro	0.8	400		400										
FeCl$_2$	0.1	Micro	6.0			600	600									
Cu(NO$_3$)$_2$.3H$_2$O	0.275	Micro	0.036		9.9											9.9
Zn(NO$_3$)$_2$.6H$_2$O	0.267	Micro	0.075											20		20
Mn.SO$_4$.H$_2$O	0.01	Micro	15.0							150			150			
total				400	9.9	4580	600	200	300	150	1850	20	900	20	4000	2030

The adsorption capacity (i.e., percentage of total elemental influx adsorbed by the resin) was tested using 18 resin columns for laboratory tests. Out of these 18 columns, 9 columns were used to mimic heat, drought, and frost conditions and 9 columns were used to test the column's capacity (Table S2). Heat, drought, and frost conditions were mimicked using 3 columns for each treatment which consisted of heating to 40˚C, drying at 20˚C to a constant weight and freezing at -19˚C for 72 hours, respectively, followed by drip-wise loading with the macro- and micro solution. The resin's capacity was simulated by dripping the macro- and the micro solutions through the resin columns using the normal concentration (3 columns and for the heat, drought and frost conditions), the double concentration (3 columns) and the triple concentration (3 columns), loading the columns up to respectively 70%, 140% and 210% of their capacity. The exchange capacity of the resin as reported by the manufacturer was ≥ 0.6 mol L^{-1} for the anion bed and ≥ 0.7 mol L^{-1} for the cation bed. Samples of the leachate were taken when all the solution was drained from the resin (after approximately 4 hours). Three resin columns loaded up to 70% of the resin's exchange capacity' were thereafter flushed with demineralized water to test the stability of the adsorption. This stability needed to be tested to check whether the ion exchange resin would release nutrients when exposed to (very) wet conditions. Furthermore, demineralized water used to clean the resin was taken as a blank sample for the adsorption test.

The recovery efficiency (i.e., percentage of total elemental flux recovered from the resin) was tested using 36 loaded resin columns in laboratory tests. In addition to these 36 loaded columns, 2 blanks were included to distinguish between the recovery efficiency of the loaded solution and background contamination from the resin or contamination caused by sample handling in the laboratory. Only the columns loaded with the double and triple concentration of the macro- and micro solutions were excluded (Table S2). All unloaded columns were, similar to the previously loaded columns, drip-wise loaded with the macro- and micro solutions. Recovery efficiency was tested using a 2M KCl extraction for NH_4^+ and NO_3^- based on previous reported high recovery rates (Fenn et al., 2002; Fenn and Poth, 2004; Fang et al., 2011; Kohler et al., 2012; Clow et al., 2015; Hoffman et al., 2019) and multiple molarities of HCl (ranging from 1 to 4M) for the other elements (Ca, Mg, K, Fe, Mn, Zn, Cu, Na, and S) since a higher recovery of the base cations was found with a 1M HCl extraction (Fenn et al., 2018) compared to a 0.5 M HCl extraction (Yamashita et al., 2014). In one test, we combined multiple molarities of HCl, resulting in an extraction sequence of 50 mL of 4M HCl, followed by 50 mL of 2M HCl, and finally an extraction with 50 mL of 1M HCl (Table 2).For both the KCl and HCl extractions, we varied the extraction volume, the extraction type, and the extraction method (Table 2). Extraction volumes used were 50 mL, 100 mL and 150 mL and extraction type was either single column extraction or batch extraction. Using the single column extraction type, the extractant was applied on the entire column while in batch extraction the resin was divided into smaller samples. These subsamples of the resin were either fresh (i.e., solution drained resin) or dried at 28 ˚C to a constant weight (Table 2). Drying of the resin facilitates subsampling and the calculation of the deposition flux. The extraction method was either drip, in which the extractant was slowly dripped over the resin, or a shake-drip combination in which the resin was shaken in 50mL of the extractant for 1 hour and the remaining extractant was dripped over the resin. For shaking, the resin was put into a 50mL centrifuge tube (Greiner bio-one) with a screw cap. Then the resin was shaken using a speed of 120 movements per minute using a GLF 3015 platform shaker at a speed of 120 movements per minute. After shaking the resin was placed back into the original tube and the extractant was allowed to drain from the resin and captured. The second 50mL followed the drip procedure. The samples of the leachate of the micro- and micro solution to load the columns, of the demineralized water to wash the loaded columns, and the samples of the extraction of the elements from the columns were analyzed. We did not filter the samples as there was no visual contamination and samples were handled under controlled laboratory conditions. Specifically, $N-NH_4^+$ and $N-NO_2 + N-NO_3^-$ concentrations were determined using a Segmented Flow Analyzer (SFA type 4000, Skalar Analytical B.V., the Netherlands), while the content of Ca, Cu, Fe, Mg, Mn, Na, total-P, S, and Zn was analyzed using the ICP-AES (Thermo-Scientific iCAP 6500 DUO, USA).

Table 2: Overview of the test for effective extraction of the ion exchanger. The KCl extraction was used for the extraction of NH_4^+ and NO_3^- while the HCl extraction is used for the extraction of Ca, Mg, K, Fe, Mn, Zn, Cu, Na, and S. The molarity of the extractant (M) was 2 for KCl and between 1-4 for the HCl extraction. In one case we used multiple molarities in one extraction, consisting of an extraction sequence of 50 mL of 4M HCl, followed by 50 mL of 2M HCl, and finally an extraction with 50 mL of 1M HCl. The single column extraction included the entire loaded column (9.8g of resin) while for batch extraction a subsample (avg. 2.5g dried resin) was used which was extracted either fresh (i.e., solution drained) or dried.

	Extraction solution		Type	Resin	Samples	Method
	M	*mL*				
KCl	2	50	Single column	Fresh	3	Drip
	2	100	Single column	Fresh	3	Drip
	2	50	Batch	Fresh	2	Drip
	2	50	Batch	Dried	2	Drip
	2	50	Batch	Dried	2	Drip
HCl	1	50	Single column	Fresh	3	Drip
	1	100	Single column	Fresh	3	Drip
	2	100	Batch	Fresh	2	Drip
	2	100	Batch	Dried	2	Drip
	2	100	Batch	Fresh	2	Shake & drip
	2	100	Batch	Dried	2	Shake & drip
	4 - 2 - 1	150	Batch	Fresh	2	Drip
	4 - 2 - 1	150	Batch	Dried	2	Drip
	2.5	100	Batch	Dried	2	Shake & drip
	3	100	Batch	Dried	2	Shake & drip
	3.5	100	Batch	Dried	2	Shake & drip

2.3 Field tests

To evaluate the accuracy of the IER-method to quantify bulk deposition and throughfall, a field study was caried out in the Netherlands (GPS 52.015745, 5.759924) in which we collected paired observations of bulk deposition and throughfall using water samples (referred to as the water-method) and the IER-method. The chosen field site consisted of a mature stand of European beech (*Fagus sylvatica*) which has been harvested at different intensities in February 2019, which resulted in four ¼-ha plots within the same stand: an unharvested control (~0% canopy openness), a high-thinning (~25% canopy openness),

a shelterwood (~75% canopy openness) and a clearcut (100% canopy openness) (Vos et al., 2023a; Vos et al., 2023b). The different harvest intensities allowed to test the method for quantifying bulk deposition and throughfall including the effect of organic substances on the performance of the IER-method. The forest stand has a temperate maritime climate with a mean annual temperature of 10.4°C and a mean annual rainfall of 805mm (KNMI, 2022). An overview of the study site characteristics and the placement of the paired samples are in table 3.

Table 3: Characterization of the study site and placement of the paired samplers in open gaps (bulk deposition) and underneath the forest canopy (throughfall). We statistically tested the behaviour of the common water method and the IER-method for throughfall and bulk deposition regardless of the forest harvest intensity treatment in which these samplers were placed.

Treatment	Canopy cover	Number of trees	Paired samplers	
	%	trees ha^{-1}	Throughfall	Bulk deposition
Control	94	245	6	1
High-thinning	72	180	5	2
Shelterwood	16	32	2	5
Clearcut	0	0	0	7

In each forest harvest treatment plot, 7 pairs of collectors were installed resulting in 28 commonly used bulk and throughfall deposition collectors (collecting the precipitation next to and below the forest) and 28 IER deposition collectors. These 7 collectors per plot collectively had a collection surface >2000cm^2 above which the reliability of the measurement is significantly increased (Bleeker et al., 2003). The collectors consisted of a polyethylene funnel mounted to a resin column, which was filled with resin for the IER-method but left empty for the water-method, and a PVC hose connecting the resin column to a polypropylene water reservoir (Fig. 2A). The funnel had a surface of 288cm^2 (including half the rim, Fig. 2B). Both the funnel and the resin column were chemically resistant and not susceptible to damage through UV-light or low temperatures. Wire couplings, in which a mesh with the size of 2mm was mounted, were used to connect the resin column to the funnel and to a hose-tail (Fig. 2C, Fig. 2D). Prior to field installation, the funnel and the resin column including the wire couplings were cleaned from chemicals loosely bound to the surface by submerging into a 0.2M HCl solution for three hours, followed by a 15-hour immersion in demineralized water which was continuously refreshed. Afterwards, the compartments were allowed to dry in a clean room and stored in clean plastic bags.
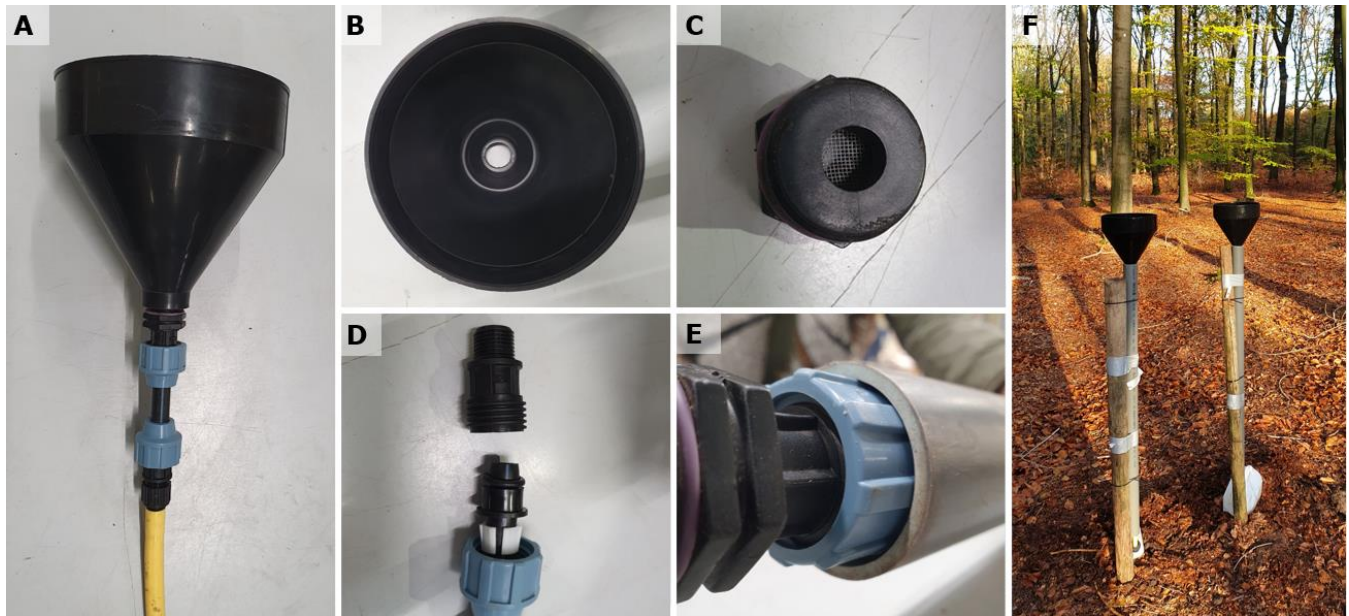
230 **Figure 2: Construction of the deposition samplers. A: the connected sampler ready for use in the field. B: the used funnel with a collection surface of 288cm². C: The wire coupling between the funnel and the resin column containing a mesh to prevent larger objects entering the resin column. D: Overview of the resin column with the wire couplings. E: the resin column fitted tightly into the PVC tube which allowed easy installation of the resin columns in the field.**

235 Field placement of the collectors was based on a digital elevation map of the canopy cover, assessed by drone-based photogrammetry (camera FC220). This digital elevation map was converted to a canopy cover map using 'reclassify' in ArcMap (version 10.6.1) in which all datapoints above 10m were assigned to be covered by canopy. Each plot was, thereafter, divided into an equal sized, seven block grid and the locations of the collectors were determined in each of these blocks using random points reflecting the canopy cover (%). Samplers were installed in the field using those random points on November

240 6th, 2019, by placing the clean, connected sampler in the holder (PVC-tube) and connecting the sample to the partly buried reservoir (Fig. 2F). The PVC tube was placed vertically so that the funnel, which was placed on top of the PVC tube, was aligned horizontal. The wire couplings of the resin column and the funnel fitted tightly into this PVC tube (Fig. 2E). Closed field blanks were installed simultaneously with the collectors, with one field blank in the clearcut (sun-exposed) and one field blank in the control (shade). Collectors and field blanks were operational for 10 weeks. Funnel contamination (leaf litter and

245 bird droppings) was recorded, and contaminated funnels were cleaned weekly. For the water-method, the leachate was collected every week and sent to the laboratory. In the laboratory, the sample volume was recorded and sample pH was measured followed by sample filtration and measurement of the concentrations of Al, Ca, Cu, Fe, K, Mg, Mn, Na, P, S and Zn using ICP-AES (Thermo-Scientific iCAP 6500 DUO, USA) and the concentrations of $N-NH_4$, $N-NO_3+N-NO_2$, and inorganic

carbon (IC) and total carbon (TC) using a Segmented Flow Analyzer (SFA 4000, Skalar Analytical B.V., the Netherlands)
250 within 24h of sampling. The volume of the leachate of the IER collectors was collected monthly, the resin columns were collected on January 14th, 2020, dried together with lab blanks to a constant weight at 28˚C and subsamples were taken for 2M KCl extraction followed by N-NH$_4$ and N-NO$_2$ + N-NO$_3$ concentration analysis using a Segmented Flow Analyzer (SFA 4000, Skalar Analytical B.V., the Netherlands) and for 3.5M HCl extraction followed by Ca, Cu, Fe, Mg, Mn, Na, P, S and Zn concentration analysis using the ICP-AES (Thermo-Scientific iCAP 6500 DUO, USA). There was no need to filter these
255 samples as there were filters around the IER and there were no visible undissolved particles. The 3.5M HCl with a volume of 100mL was chosen as an extractant because reasonable extraction efficiency for P combined with reasonable extraction efficiencies for the other elements (except Zn). As a result of contaminations by bird faeces, only 18 out of the 28 paired collectors were used for the comparison. Uncontaminated paired collectors were evenly distributed between throughfall and bulk deposition.

260

2.4   Calculations and statistical analysis

The concentrations of the resin columns used within the laboratory and field test were corrected for the subsampling in case of batch extraction, corrected for field- and lab blanks and corrected for sample dilution prior to chemical analysis. To correct for subsampling, the concentration of the subsample was multiplied by the concentration of the entire column based on the
265 weights of the subsample and the entire column respectively. Concentrations of the field and lab blanks were subtracted from the concentrations of the entire column to correct for field and lab contamination. For the bulk deposition samplers in the forest gaps the sunlight exposed field blank was used, for the throughfall samplers underneath the forest canopy, the shadow field blank was used. Subsequently, the concentrations of the resin columns used within the field test were converted to the amounts per ha^{-1} for the entire measurement period. Thereafter, the deposition in kg ha^{-1} was calculated based on the funnels surface.
270 For the water-method, the precipitation in L ha^{-1} was calculated based on the water volume per funnel (mL). Then the measured weekly concentrations were converted to kg L^{-1} and multiplied with the precipitation (L ha^{-1}). Finally, for both methods, the samples were checked for bird droppings based on the P content, and samples with a P influx (in kg ha^{-1}) larger than the mean plus the 2 times the standard deviation were removed.

For the laboratory test, we calculated the adsorption capacity and the recovery efficiency. The adsorption capacity (i.e.,
275 percentage of total elemental influx adsorbed by the resin) was calculated as:

$$Adsorption\ capacity = \left(1 - \left(\frac{A_{out}}{A_{in}}\right)\right) * 100$$

In which A_{in} is the total amount of macro and micronutrients in the solution (in µmol) applied to the resin and A_{out} is the amount in the leachate (in µmol). The recovery efficiency (i.e., percentage of total elemental flux recovered from the resin) was calculated as:

$$Recovery\ efficiency = \frac{A_{ex}}{A_{in}} * 100$$

In which A_{ex} is the amount of macro and micronutrients in the leachate applied extract (in µmol) which was poured over the loaded resin.

The adsorption capacity of the resin was evaluated using the Wilcoxon signed rank test to test the hypothesis that adsorption is equal to 100%. This test was applied only when the observed adsorption capacity was below 100% to address the issue of ties. Recovery efficiencies of lab extractions differing in molarity, resin pre-treatment and extraction type was tested using ANOVA type I error for unbalanced data following construction of a generalized least squares model. Heterogeneity between groups was overcome using the varIdent weighting from the R package "*nlme*". Tukey's post-hoc (HSD) test was performed following ANOVA using the R package "*emmeans*" to test for differences between groups. Goodness of fit between the original and the IER-method of the field test were tested using linear models using the *lm* function in the *lme4* package (Bates et al., 2014). Outliers were removed from the linear models when the Cook's distance was larger than 4/n in which n is the number of observations. The funnel position (throughfall or bulk deposition) was added as a random effect using *lme* models. This random effect was retained only if it improved model performance by Δ2, following Zuur et al. (2009), which proved to be true for none of the models.

3   Results

3.1   Adsorption capacity

The adsorption capacity of the resin (i.e., % of elemental flux bound to the resin) when loaded up to 70% of the resins exchange capacity was 100% for all nutrients, with only Na and P being slightly lower (96-97%) (Table 4). The adsorption capacity was not influenced by the flushing of the resin with demineralized water indicating that the elements once adsorbed are not released through an excess of water like heavy precipitation.

Overloading the resin up to 150% of the cation bed capacity resulted in decreased adsorption of Na>NH_4^+>K and a maximum loading of the cation bed of 115%. Overload of the anion bed up to 160% decreased the adsorption of P>NO_3^-. Increasing the elemental flux over the resin up to 230% of the cation bed capacity and 240% of the anion bed capacity resulted in lower adsorption of almost all elements except Ca and Zn (Table 4). Lab-controlled environmental conditions mimicking heat, drought and frost reduced the adsorption capacity of Na and P, and heat and drought slightly lowered the adsorption capacity

305 of NH_4^+. Elemental adsorption within the resins exchange capacity was thus close to 100% for all elements when the resin was used within its capacity, except for P, which was underestimated under the different simulated environmental conditions.

Table 4: The mean ± s.e. of the adsorption capacity of the ion exchange resin following different tests (n = 3). Adsorption capacity is expressed as a % of the total elemental content that was captured by the resin. Tests included the loading of the resin with known concentrations within the resins capacity (leachate), loading the resin beyond the resins capacity (150% - 160% of respectively cation and anion bed and 230% - 240% of respectively the cation and anion bed), and resin pre-treatments including warmth, drought, and frost. For adsorption capacities <100% we performed a Wilcoxon signed rank test (WSRT) to see if these elements were different from a 100% adsorption. The elements included in this test are marked in bold, and the number of samples used for the Wilcox test, the V and P values are given.

Test	Ca	Cu	Fe	K	Mg	Mn	Na	P	S	Zn	NH₄⁺	NO₃⁻	WSRT n	WSRT P
70% loading	100 ± 0.0	100 ± 0.05	100 ± 0.034	100 ± 0.0	100 ± 0.09	100 ± 0.013	**97 ± 0.31**	**96 ± 0.48**	100 ± 0.0	100 ± 0.025	**99 ± 0.13**	100 ± 0.012	9	0.009
150-160% loading	100 ± 0.1	**99 ± 0.067**	100 ± 0.071	**85 ± 3.7**	100 ± 0.15	100 ± 0.14	**66 ± 2.9**	**59 ± 2.0**	**99 ± 0.31**	**99 ± 0.11**	**74 ± 4.4**	**93 ± 3.2**	24	< 0.001
230-240% loading	**99 ± 0.068**	**99 ± 0.094**	**99 ± 0.18**	**63 ± 0.87**	**97 ± 0.098**	**99 ± 0.13**	**53 ± 0.4**	**65 ± 1.5**	**86 ± 0.67**	**99 ± 0.097**	**57 ± 0.94**	**74 ± 0.71**	36	< 0.001
Heat	100 ± 0.0	100 ± 0.0	100 ± 0.011	100 ± 0.0	100 ± 0.0	100 ± 0.018	**96 ± 1.4**	**77 ± 5.3**	100 ± 0.012	100 ± 0.0	**98 ± 0.72**	100 ± 0.012	9	0.004
Drought	100 ± 0.2	100 ± 0.05	100 ± 0.011	100 ± 0.0	100 ± 0.045	100 ± 0.015	**96 ± 1.1**	**79 ± 3.9**	100 ± 0.0	**99 ± 1.1**	**98 ± 0.69**	100 ± 0.022	12	0.004
Frost	100 ± 0.0	100 ± 0.05	100 ± 0.011	100 ± 0.0	100 ± 0.0	100 ± 0.004	**97 ± 0.12**	**81 ± 3.6**	100 ± 0.012	100 ± 0.0	**99 ± 0.086**	100 ± 0.012	9	0.009

315

3.2 Recovery efficiency

The recovery efficiency of NH_4^+ and NO_3^- under laboratory conditions (i.e., % of the elements that can be extracted from the resin) was generally high (mostly 90-100%) with recovery depending on the molarity of the extraction (Table 5). The recovery efficiency of NH_4^+ and NO_3^- was weak but significantly higher with 1M KCl as an extractant compared to 2M KCl (Anova, 320 F-value: 4.4, P-value: 0.048, Df: 22). We did not find differences between fresh or dry resin, or between drip or shake-drip treatments using KCl extractions.

The average recovery efficiency following HCl extraction was high (>90%) for Ca, K, Na and Mn, slightly lower (>80%) for Mg, S, Cu and Fe, relatively low for P (40-91%) and very low (6-25%) for Zn (Table 5). Because extraction of Zn was

unreliable, this element is not further included in average recovery numbers. The highest average recovery efficiencies were achieved with dried resin using either 2M HCl extraction or 4-2-1M HCl extraction. Specifically, the 2M HCl methods yielded average recovery efficiencies of 94% (drip) and 100% (shake-drip), while the 4-2-1M HCl method on dried resin achieved 90% recovery efficiency. Recovery efficiency was significantly higher following an extraction on dried resin (avg. recovery 88%) compared to fresh resin (avg. recovery 80%), and recovery efficiency was slightly higher following a shake-drip treatment (avg. recovery 87%) compared to drip only treatment (avg. recovery 84%) (table S3). We found an interaction effect between elements and pre-treatment, elements and molarity and elements and extraction type, indicating that different elements responded differently to the different treatments. Overall, highest average recoveries using HCl were found for the 2M dry weight shake and drip treatment, resulting in an average recovery of 100% whereas lowest average recoveries (72%) were found for the 1M fresh weight drip treatment (Table 5).

3.3   Performance under field conditions

There was a positive significant linear relationship between the deposition estimates of the water-method and the IER-method for all elements except for Ca, Zn and Fe (Table 6, Fig. 3). Absence of a relation for Ca, Zn and Fe was not related to the correction for contamination in blanks and for the lab-recovery (Table 6).

The IER data corrected for contamination of blanks and the lab-recovery overall resulted in the highest R^2-adjusted, resulting in a corrected goodness of fit up to 0.96 (K) and between 0.8 to 0.9 for NH_4^+, NO_3^-, S, Mg, and Mn (Table 6). There was no difference between throughfall and bulk deposition between the IER-method and the water method. For none of the elements, adding the position of the funnel (either throughfall or bulk deposition) increased the performance (expressed as AIC) of the statistical model. The IER-method tended to have lower deposition estimates in the bulk deposition for Mg, Mn, Na and S, but overall, the IER-method resulted in higher deposition estimates for NH_4^+, K, S, NO_3^-, Mg, Mn, and Na compared to the water-method (Fig. 3). For Fe, P, and Cu, for which the water-method yielded higher deposition estimates, all values of the water-method were below detection limit (Table S4).

350

Table 5: Recovery efficiency of Ca, Cu, Fe, K, Mg, Mn, Na, P, S and Zn following HCl extractions and of NH_4^+ and NO_3^- following KCl extractions. Recovery efficiencies are expressed as a % of the total elemental content poured over the resin. The efficiencies of the recovery were tested using extractions with different molarities (Mol), based on fresh (FW) or dried (DW) resin and based on drip or shake-drip treatments. The number of samples (n) for each extraction combination, the average arithmetic recovery per extraction combination (Avg) and the average arithmetic recovery for each element is given. Recovery percentages per element closest to 100 are indicated in bold. Differences in recovery efficiencies between elements is indicated with small capital letters based on the average element recovery, test statistics are given in Table S3.

355

Mol	Resin	Method	n	Ca	Cu	Fe	K	Mg	Mn	Na	P	S	Zn	Avg*	NH_4^+	NO_3^-
1	FW	Drip	6	30 ± 5.2	80 ± 6.3	56 ± 4.2	88 ± 1.1	59 ± 4.5	91 ± 6.5	97 ± 3.0	59 ± 6.5	92 ± 2.2	17 ± 3.6	72	**100** ± 1.9	**98** ± 5.0
2	DW	Drip	2	130 ± 3.8	94 ± 1.3	99 ± 0.05	**100** ± 3.4	98 ± 6.8	**100** ± 1.8	93 ± 3.3	40 ± 9.7	91 ± 5.2	21 ± 6.0	94	97 ± 6.0	94 ± 3.9
2	DW	Shake-Drip	2	130 ± 9.0	**100** ± 2.6	110 ± 3.5	110 ± 1.7	**100** ± 3.7	110 ± 2.4	**100** ± 4.0	65 ± 16	**100** ± 6.1	7.6 ± 0.45	100	94 ± 9.0	89 ± 12
2	FW	Drip	2	85 ± 2.1	81 ± 0.45	88 ± 1.5	86 ± 5.0	84 ± 6.2	91 ± 1.7	82 ± 5.8	43 ± 9.2	96 ± 3.5	25 ± 10	82	80 ± 6.1	95 ± 8.1
2	FW	Shake-Drip	2	82 ± 11	80 ± 8.6	87 ± 6.2	87 ± 8.6	81 ± 13	88 ± 9.0	84 ± 8.4	69 ± 19	93 ± 5.1	5.4 ± 0.45	83		
2.5	DW	Shake-Drip	2	86 ± 1.2	78 ± 0.65	72 ± 0.60	**100** ± 3.1	85 ± 4.5	81 ± 0.20	**100** ± 1.3	91 ± 0.70	78 ± 11	6.1 ± 0.4	86		
3	DW	Shake-Drip	2	82 ± 5.6	71 ± 6.3	67 ± 8.9	98 ± 6.9	77 ± 9.1	77 ± 7.8	99 ± 2.8	84 ± 1.5	70 ± 1.2	6.1 ± 0.6	81		
3.5	DW	Shake-Drip	2	99 ± 0.0	89 ± 0.45	80 ± 1.9	88 ± 8.1	93 ± 1.9	96 ± 2.4	84 ± 5.2	83 ± 4.1	83 ± 6.9	11 ± 2.6	88		
4-2-1	DW	Drip	2	**100** ± 11	92 ± 6.4	99 ± 3.6	93 ± 5.0	88 ± 5.8	**100** ± 6.6	89 ± 7.5	49 ± 5.5	96 ± 3.1	31 ± 5.8	90		
4-2-1	FW	Drip	2	86 ± 0.75	85 ± 0.55	90 ± 2.9	**100** ± 23	80 ± 1.9	92 ± 0.60	82 ± 1.6	49 ± 0.60	97 ± 3.6	**44** ± 10	85		
		Arithmetic average		91[d]	83[bc]	83[c]	93[ab]	84[c]	91[b]	90[a]	63[e]	88[b]	19[f]			

*Average without Zn as this element was unreliable using our extraction method.

360
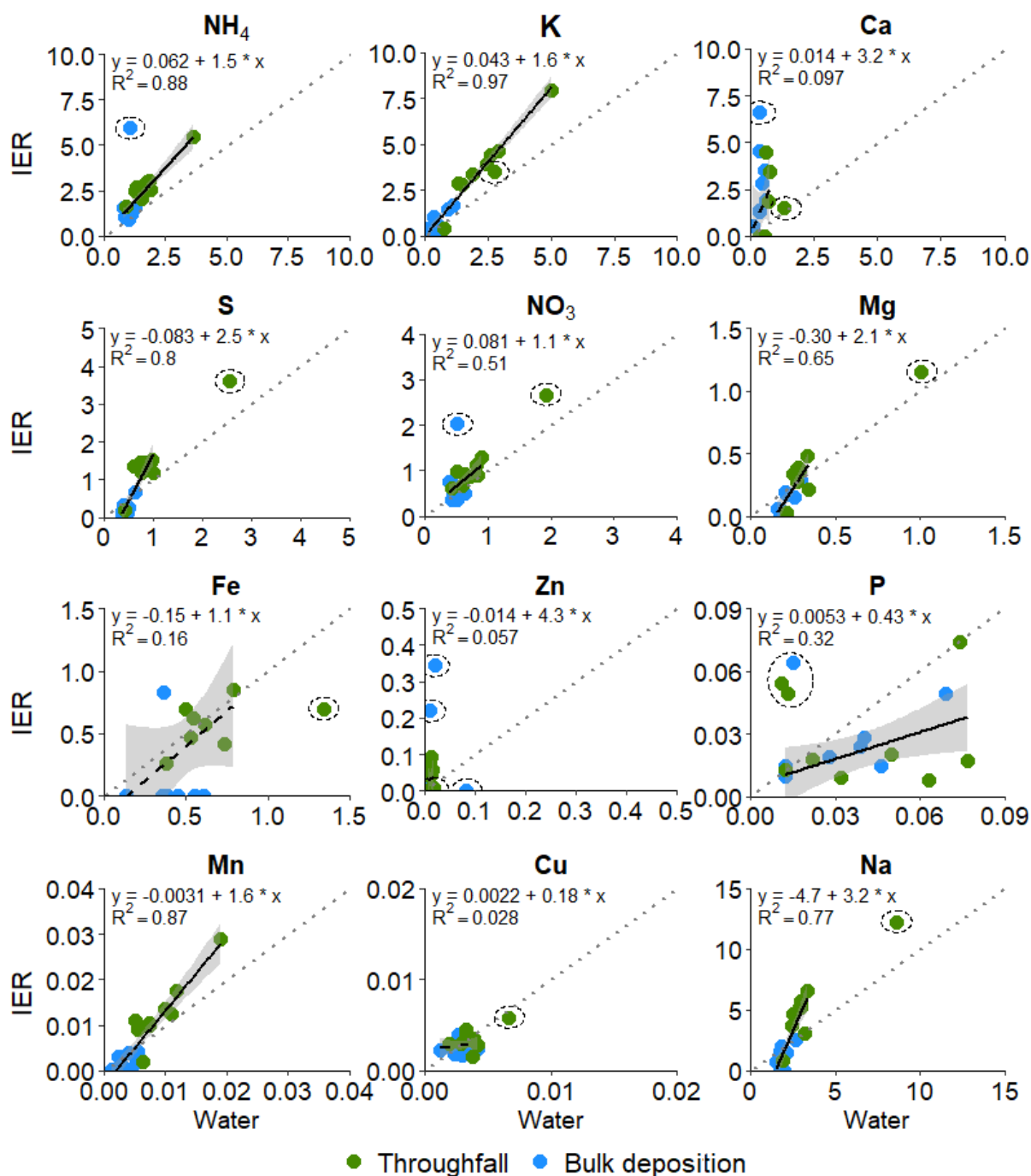
Figure 3: Relationship between the deposition estimates of the IER-method (kg ha⁻¹) and of the water-method (kg ha⁻¹) for the 10-week measurement period. Significant relationships are depicted with a solid black line, non-significant relationships with the dashed black line. The regression formula, the 95% confidence intervals (grey) and the R² are shown. The standard errors and significance of the intercept and slope are given in table 6 . The 1:1 line is shown as the dotted grey line.

Table 6'': **Regression Coefficients (Intercept and Slope ± s.e.) and R^2 of models for the relation between the IER Method and the commonly used method, including correction for blanks and lab recovery (n = 18). Differences between corrected, blank corrected and recovery corrected is related to the corrections for contaminations (blank corrected) and for the recovery of the elements (recovery corrected). The corrected shows the data which is corrected for both the contamination and the recovery. The R^2-adj. of the model with the best fit is highlighted in bold. For each model we calculated the mean absolute error (MAE) using this formula: MAE = (1/n) * Σ|yi – xi|. The MAE is the average absolute difference between the predicted and the observed IER data.**

		NH_4^+	NO_3^-	S	P	K	Ca	Mg	Mn	Cu	Fe	Zn	Na
Corrected	Intercept	0.062 ±	0.081 ±	-0.83 ±	0.0053 ±	0.043 ±	0.014 ±	-0.30 ±	-0.0031 ±	0.0022 ±	-0.15 ±	-0.014 ±	-4.7 ±
	s.e.	$0.21^{n.s.}$	$0.18^{n.s.}$	0.20^{***}	$0.0078^{n.s.}$	$0.13^{n.s.}$	$1.4^{n.s.}$	0.099^{**}	0.0012^{*}	0.00085^{*}	0.35	$0.057^{n.s.}$	1.1^{***}
	Slope	1.5 ±	1.1 ±	2.5 ±	0.43 ±	1.6 ±	1.1 ±	2.1 ±	1.6 ±	0.18 ±	1.1 ±	4.3 ±	3.2 ±
	s.e	0.14^{***}	0.30^{**}	0.31^{***}	0.17^{*}	0.069^{***}	1.6	0.40^{***}	0.15^{***}	$0.27^{n.s.}$	$0.69^{n.s.}$	$5.0^{n.s.}$	0.45^{***}
	R^2	**0.88**	0.51	**0.80**	**0.32**	**0.96**	0.097	**0.65**	**0.87**	0.028	**0.16**	**0.057**	**0.77**
	MAE	0.31	0.16	0.19	0.0096	0.25	1.3	0.067	0.0021	0.00065	0.30	0.029	0.84
Blank cor.	Intercept	0.11 ±	-0.099 ±	-1.39 ±	0.086 ±	0.36 ±	-1.1 ±	-0.50 ±	-0.0049 ±	0.0066 ±	-0.0044 ±	0.014 ±	-8.0 ±
	s.e.	$0.18^{n.s.}$	$0.13^{n.s}$	0.50^{*}	0.035^{*}	$0.30^{n.s}$	$3.5^{n.s}$	$0.27^{n.s}$	$0.0031^{n.s}$	0.0014^{**}	$0.018^{n.s}$	$0.016^{n.s}$	2.6^{**}
	Slope	1.1 ±	0.83 ±	5.2 ±	-0.25 ±	4.2 ±	11 ±	4.7 ±	4.3 ±	0.31 ±	0.061 ±	-0.055 ±	6.6 ±
	s.e.	0.12^{***}	0.23^{***}	0.8^{***}	$0.81^{n.s}$	0.17^{***}	$7.0^{n.s}$	1.1^{***}	0.43^{***}	$0.60^{n.s}$	$0.03^{n.s}$	$1.4^{n.s}$	1.2^{***}
	R^2	0.82	0.46	0.72	0.00	**0.97**	**0.14**	0.50	0.85	0.015	0.15	0.00	0.66
	MAE	0.29	0.13	0.60	0.058	0.67	3.6	0.21	0.0063	0.0016	0.017	0.0099	2.5
Recov. Cor.	Intercept	0.15 ±	0.15 ±	0.070 ±	0.0053 ±	0.043 ±	2.0 ±	0.10 ±	0.00087 ±	0.0022 ±	0.020 ±	0.055 ±	-0.44 ±
	s.e.	$0.22^{n.s}$	$0.17^{n.s}$	$0.17^{n.s}$	$0.0078^{n.s}$	0.13	1.8^{*}	$0.10^{n.s}$	$0.0011^{n.s}$	0.00085^{*}	0.0091^{*}	0.063	$1.0^{n.s}$
	Slope	1.5 ±	1.1 ±	1.6 ±	0.43 ±	1.6 ±	3.5 ±	1.3 ±	1.3 ±	0.18 ±	-0.0040 ±	1.4 ±	1.9 ±
	s.e.	0.14^{***}	0.29^{***}	0.26^{***}	0.17^{*}	0.069^{***}	3.5	0.41^{**}	0.15^{***}	$0.27^{n.s}$	0.018	5.5	0.43^{***}
	R^2	**0.88**	**0.51**	0.73	**0.32**	**0.97**	0.07	0.39	0.84	0.028	0.00	0.00	0.57
	MAE	0.32	0.15	0.16	0.0096	0.25	1.7	0.068	0.0018	0.00065	0.0074	0.03	0.69

*** < 0.001; ** 0.01 >< 0.001; * 0.05 <> 0.01; no star is not significant; [1] log transformed values.

4   Discussion

4.1   Adsorption capacity

We aimed to test the capacity of IER as a method to quantify atmospheric deposition for a broad range of macro- and micro-
375   elements, comparing results under laboratory and field conditions and in the latter case comparing bulk deposition and
throughfall. First, the adsorption capacity of the IER, when loaded up to 70% of its capacity as reported by the manufacturer,
was generally high for all elements. High adsorption confirms earlier studies who found no elemental loss of NO_3^-, NH_4^+ and
SO_4 (Simkin et al., 2004; Sheibley et al., 2012; Sheng et al., 2013) or only slight losses of NH_4^+ and NO_3^- (Fang et al., 2011)
and contradicts findings of low resin adsorption (Langlois et al., 2003). We show that IER is also able to adsorb above 99%
380   for a range of other elements, including the base cations and some micronutrients, and that the adsorbed elements are not
released in response to an excess of water such as heavy precipitation. Therefore, IER can be loaded within the 70% of its
exchange capacity without risking lower elemental adsorption. However, slightly lower adsorption capacities were found for
Na and P. These lower adsorption capacities are caused by the lower cation-exchanger affinity for Na^+ and lower anion-
exchanger affinity for HPO_4^{2-} (Skogley and Dobermann, 1996; Park et al., 2014). The lower adsorption capacities when using
385   the resin within its capacity can lead to an underestimation of the total deposition of P by 4%, although other studies report no
lower adsorption capacities for P (Tahovská et al., 2016). Despite the possible underestimation of the total deposition, studies
using IER report P deposition values within the natural ranges (Decina et al., 2018; Hoffman et al., 2019), indicating that the
method usually also works well for P. The lower adsorption capacity of Na, however, can result in lower estimates of the
deposition for multiple elements when Na is used as an tracer for canopy exchange processes (Staelens et al., 2008), and the
390   use of Na as a tracer in IER-deposition studies is thus questionable.

To further test the affinity of the resin for the studied elements, the resin was loaded to approximately 160% and 240% of its
capacity. Based on the adsorption capacity beyond the resins capacity, we found that the cation bed has an affinity of Ca = Fe
> Cu = Mn = Zn > Mg > K > NH_4^+ > Na which is in line with the previous reported resin affinity (Skogley and Dobermann,
1996). The anion bed has an affinity of S > NO_3^- > P which agrees with earlier studies (Skogley and Dobermann, 1996; Park
395   et al., 2014). The resins affinity and the adsorption capacity for different levels of loading beyond the resins capacity is of
importance for resin columns under suspicion of overloading. We did not find lower adsorption of Ca and Fe and only slightly
lower adsorption of Cu, Mg, Mn and Zn, indicating that, when columns are slightly overloaded, these estimates are still reliable.
When columns are loaded > 100% of the capacity, the estimates for K, Na, P, S, NH_4^+ and NO_3^- are not reliable. Therefore, in
case of suspicion of ion exchange overload, tests are recommended to check if stoichiometry between any element of Ca, Cu,
400   Mg, Mn and Zn with K, Na, P, S, NH_4^+ and NO_3^- falls within the stochiometric range of natural deposition estimates. We
strongly recommend to collect the resin columns prior to resin saturation as adsorption of Na and P can further decrease when
saturating the resin up to 90 or 100%. The time period that the resin can stay in the field depends on the total atmospheric

deposition and the volume of resin used. For remote areas with low deposition levels and low risk of sample contamination (e.g. by bird feces) the resin can stay for multiple months up to a year in the field as long as adequate resin volumes are used.

405   Heat, drought and frost treatments hardly influenced the absorption capacity of most elements, but decreased the P adsorption capacity and, in case of heat and drought, NH_4^+ and Zn (the latter only for drought) adsorption. These findings are in line with the adsorption behavior of some other IER types, where drying significantly reduced NH_4^+ adsorption while frost-thaw cycles did not (Hart and Binkley, 1984; Kjonaas, 1999). However, in other work extensive dry-wet cycles did not affect the adsorption of PO_4, NO_3^- and NH_4^+ (Mamo et al., 2004) indicating that the effect of environmental conditions differs per resin type.

410   Application of the IER-method without an adsorption pre-test of the resin can therefore potentially underestimate NH_4^+ and P deposition when used in areas with temperatures above 40˚C and can potentially underestimate NH_4^+, P and Zn deposition in areas with longer drought periods. Despite the effect on some elements, weather circumstances generally seem to have little effect indicating that the method is suitable under different climatic circumstances, like the boreal zone (Fenn et al., 2015), temperate zone (Fenn and Poth, 2004; Hoffman et al., 2019) and the tropics (Kohler et al., 2012; Ibrahim et al., 2022). The

415   robustness of the method under different climatic circumstances implies that it can be used to compare deposition over large environmental gradients, which is essential to understand regional and global deposition patterns.

4.2   Recovery efficiency

The recovery efficiency was tested based on differences in molarity, resin pre-treatment and extraction type. For this test, we

420   used generally double or triple samples which can be considered as a low sample size. However, because these tests were performed under controlled laboratory conditions, a small sample set can be justified. When using the ion exchange resin method for field studies, we recommend testing the extraction solution for a larger number of samples to reduce the standard error (table 5). Nonetheless, we are confident that our conclusions are justified, given the controlled circumstances of the laboratory tests and the relatively low standard errors.

425   Recovery of NH_4^+ and NO_3^- was highest following a 1M KCl extraction based on controlled percolating of the extraction solution through the resin. Although highest recovery following a 1M KCl extraction was reported before (Hart and Binkley, 1984), most studies indicate that 2M KCl extractions will lead to higher recovery of both NO_3^- and NH_4^+ (Kjonaas, 1999). However, the 2M KCl recovery efficiencies of this study were comparable to other studies using 2M KCl as an extractant (Fenn et al., 2002; Sheng et al., 2013; Tulloss and Cadenasso, 2015). The highest recoveries were obtained by using dried resin

430   and the combined shake-drip methods.

Recovery efficiency following HCl extraction differed between elements and depended on the extraction itself. We choose HCl as an extractant as this extraction solution allows measurements of a broad range of elements on the ICP-AES and this method was rarely tested. A limited number of studies used HCl as an IER extractant (Van Dam et al., 1987; Dobermann et al., 1997; Szillery et al., 2006; Yamashita et al., 2014) but only one study, testing only two elements, reported (high) elemental

435   recoveries (Van Dam et al., 1987). Although H^+ has a relatively low affinity for the cation bed (Skogley and Dobermann,

1996), we expected that increasing molarities would increase recovery efficiency of both the cation and the anion bed. Surprisingly, recovery efficiency was highest using 2M HCl and 4-2-1M HCl, although highest recovery differed between elements (Table 5). Overall, we did find much higher recovery efficiencies for Ca and Mg using HCl extractions compared to KI and H_2SO_4 extractions (Kohler et al., 2012; Wieder et al., 2016), which can be related to a better extraction efficiency of

440 HCl. Absence of higher recoveries using > 3M HCl can be caused by differences in extraction time between treatments (Zarrabi et al., 2014) although the overall differences in recovery efficiencies between extractants were rather small.

Recovery efficiency was higher when resin was dried prior to HCl extraction and when using the shake-drip extraction (Table S5 and S7). The mechanism behind higher recovery efficiency following pre-extraction drying remains speculative but might be related to a better accessibility of the extract to reach micropores when the resin was dried. Previously, it was argued that

445 pre-loading drying resulted in lower recovery efficiencies because of unavailable micropores due to swelling of the resin after rewetting (Kjonaas, 1999) but this unavailability of micropores was contradicted by Mamo et al. (2004) who found that dry-wet cycles significantly increased the desorption of elements from the resin. Occurrence of dry-wet cycles under field conditions can therefore interfere with the recovery efficiency of elements from the resin which could possibly bias deposition estimates. This effect is, however, likely small as full drying resulted in only 8% more efficient recoveries. The higher recovery

450 following shake-drip treatment can result from longer contact time with the extractant (Zarrabi et al., 2014) while still avoiding the equilibrium reaction which occurs when using the shake treatment only. However, the present paper was not designed to test the effect of extraction time on the recovery efficiency, a complete test of this hypothesis will have to await future experimentation.

Finally, the best extraction to use depends on the elements of interest. When studied elements are limited to the base cations,

455 the 2M HCl extraction provides good recovery efficiencies. However, studies including P and Zn should rather choose for a HCl extract with a higher molarity or choose another extractant. Overall, recovery efficiencies of P and Zn were rather low, which may result from the low initial concentrations (Zarrabi et al., 2014). We did not test for different extraction solutions as there are only limited options for extracting a broad range of macro- and micro-solutions. However, for P and Zn different extraction solutions should be tested to increase the recovery efficiency. Furthermore, using the recovery efficiencies, we found

460 only limited evidence of a release of background levels of elements from the resin. Indications of the release of background levels were present for Ca (up to 130% recovery) and Na (up to 110% recovery). These indications were mainly present in the 2M HCl dry weight shake-drip extraction and could possibly be caused by lab contaminations. We did not find evidence for high background levels of NO_3^- and NH_4^+, contrary to Langlois et al. (2003) who argued that the IER-method was not suited for monitoring subtle patterns of NO_3^- and NH_4^+ deposition. Together, our findings indicate that both KCl and HCl perform

465 well as an extractant except for P and Zn for which new extraction methods should be tested.

4.3 Performance under field conditions

In general, deposition estimates based on the IER-method were positively related to the deposition estimates of the water-method, however, the IER-method often resulted in higher deposition estimates. Exceptions were Fe and Ca, for which we did not find a relation between the deposition estimates of the IER-method and the water-method. This could indicate pollution related to elevated Ca and Fe leaching from the sample materials. For example, in the sun-exposed field blank we found high Fe pollution causing the Fe deposition levels of all exposed collectors to be 0 (Fig. 3). For the collectors corrected for the shade-exposed field blank, we found good agreement between the deposition estimate of the IER-method (0.68 kg ha^{-1} $\pm$ 0.12 s.e.) and the water-method (0.66 kg ha^{-1} $\pm$ 0.09 s.e.) with the deposition estimates of both methods within the normal range of throughfall Fe deposition of the winter period (RIVM, 2015). For Zn we found much higher deposition values using the IER-method compared to the water-method in contrast to throughfall which was much higher than bulk deposition estimates multiplied by the throughfall multiplication factor (Table S1). It could be that the presence of organic particles interfered with the recovery efficiency of Zn, possibly leading to an overestimation of the Zn throughfall.

The higher deposition estimates of the IER-method compared to the water-method for NH_4^+ and NO_3^- can be caused by absence of biochemical reactions which causes losses of these elements in the original samplers (Fenn and Poth, 2004; Kohler et al., 2012). Higher deposition estimates using the IER-method can also be related to the low concentration of elements in the water-method, which were often below detection limit (Table S4). Overall, slightly higher deposition values using IER columns were reported before (Fenn and Poth, 2004; Simkin et al., 2004; Kohler et al., 2012). Because of absence of biochemical reactions and higher reliability of the lab measurements for IER-samples, the IER-method is likely more reliable to quantify both bulk deposition and throughfall compared to the water-method and the generally higher deposition estimates are likely a better representation of the actual atmospheric deposition.

The lower deposition estimates of P can be caused by a better adsorption of inorganic P compared to organic P to the resin (Zarrabi et al., 2014) which potentially reduces the recovery efficiency of P under field-conditions compared to lab-conditions. However, additional field tests are necessary for P to compare the difference between field and laboratory adsorption and recovery efficiencies. In this test, we attempted to extract PO_4^{3-} from the resin using 2M KCl as an extractant but achieved only an 8% recovery (n = 4, data not shown). To determine if the lower deposition estimates of P are due to better adsorption of inorganic P compared to organic P, further efforts are needed to successfully extract PO_4 from the resin. For other elements, the comparison of the IER-method and the water-method did not give evidence of lower adsorption or recovery efficiencies under field conditions. Absence of this effect might, however, be related to the winter-period in which the field measurements took place as, for example, pollen were hypothesized to reduce recovery of NH_4^+, NO_3^- and SO_4 from the IER (Brumbaugh et al., 2016). Lower field recovery might therefore, beside the resin type and the extraction method, be related to the amount of organic particles like pollen which was not included in this study.

5 Conclusions

500 We tested the suitability of the IER-method for quantifying bulk deposition and throughfall of macro- and micronutrients by assessing adsorption capacities and recovery efficiencies under controlled laboratory conditions, followed by an evaluation of the performance of the method under field conditions.

Results showed that (1) the adsorption capacity of the resin under controlled laboratory conditions was close to 100% for all nutrients; (2) Extraction using KCl (1 or 2 M) is effective for nitrogen (NH_4^+ and NO_3^-) with general high recoveries (mostly 505 90-100%) depending on the molarity of the extraction, while extraction using HCl is effective for Ca, K, Na, Mn, Mg, S, Cu and Fe but not for P and Zn for which testing other extraction methods or extraction solutions is recommended; (3) drying the resin prior to extraction and using a shake-drip extraction method increased the recovery efficiencies; (4) the IER-method is useful under a broad range of environmental conditions, since heat (40°C), drought and frost (-15°C) hardly affected the adsorption of nutrients except for P which was reduced up to 25%; and (5) the IER-method performed well under field 510 conditions, resulting in similar but consistent higher deposition estimates compared to the water method.

Our results even imply a higher reliability of the IER-method than the water method under certain circumstances since uncertainties related to biological reactions and the detection limit for lab measurements could be removed. However, possible contamination of the IER collectors due to factors such as bird faeces or other animal disturbances is a point of concern, as long field exposure increases the risk of contamination. It is therefore recommended to increase the number of samplers when 515 using the IER method. We conclude that IER is a powerful tool for the monitoring the element input by bulk deposition and throughfall for of a broad range of elements, across a broad range of environmental conditions.

Author contributions

Marleen A.E. Vos, conceived the ideas and designed the methodology. Prior to testing the methods, the ins and outs were discussed with W. de Vries and F.J. Sterck. Marleen A.E. Vos tested the Ion Exchange Resin method both in the laboratory 520 and in the field, prepared the samples for chemical analysis which was ultimately performed by the laboratory staff. Statistical analysis was performed by Marleen A.E. Vos. Marleen A.E. Vos led the writing of the manuscript. All authors contributed critically to the drafts and gave final approval for publication.

Data availability statement

No data has been published yet. Data will be made available upon request.

525 ## Competing interest

The authors have no conflicts of interest to declare that are relevant to the content of this article.

Literature

Balestrini, R., Arisci, S., Brizzio, M.C., Mosello, R., Rogora, M., Tagliaferri, A., 2007. Dry deposition of particles and canopy exchange: Comparison of wet, bulk and throughfall deposition at five forest sites in Italy. Atmos Environ 41, 745-756.

Bates, D., Mächler, M., Bolker, B., Walker, S., 2014. Fitting linear mixed-effects models using lme4. arXiv preprint arXiv:1406.5823.

Bayar, S., Fïl, B.A., Boncukcuoglu, R., Yilmaz, A.E., 2012. Adsorption kinetics and isotherms for the removal of zinc ions from aqueous solutions by an ion-exchange resin. Journal of the Chemical Society of Pakistan 34, 841.

Bleeker, A., Draaijers, G., van der Veen, D., Erisman, J.W., Mols, H., Fonteijn, P., Geusebroek, M., 2003. Field intercomparison of throughfall measurements performed within the framework of the Pan European intensive monitoring program of EU/ICP Forest. Environ Pollut 125, 123-138.

Boutin, M., Lamaze, T., Couvidat, F., Pornon, A., 2015. Subalpine Pyrenees received higher nitrogen deposition than predicted by EMEP and CHIMERE chemistry-transport models. Scientific reports 5, 1-9.

Bowman, W.D., Cleveland, C.C., Halada, Ĺ., Hreško, J., Baron, J.S., 2008. Negative impact of nitrogen deposition on soil buffering capacity. Nature Geoscience 1, 767-770.

Brumbaugh, W.G., Arms, J.W., Linder, G.L., Melton, V.D., 2016. Development of ion-exchange collectors for monitoring atmospheric deposition of inorganic pollutants in Alaska parklands, US Geological Survey.

Cerón, R.M., Cerón, J.G., Muriel, M., Rangel, M., Lara, R.d.C., Tejero, B., Uc, M.P., Rodríguez, A., 2017. Assessing the Impact of Sulfur Atmospheric Deposition on Terrestrial Ecosystems Close to an Industrial Corridor in the Southeast of Mexico. Journal of Environmental Protection 8, 1158.

Clow, D.W., Roop, H.A., Nanus, L., Fenn, M.E., Sexstone, G.A., 2015. Spatial patterns of atmospheric deposition of nitrogen and sulfur using ion-exchange resin collectors in Rocky Mountain National Park, USA. Atmos Environ 101, 149-157.

de Vries, W., Erisman, J.W., Spranger, T., Stevens, C.J., van den Berg, L., 2011. Nitrogen as a threat to European terrestrial biodiversity. The European nitrogen assessment: sources, effects and policy perspectives, 436-494.

de Vries, W., Posch, M., Reinds, G.J., Hettelingh, J.-P., 2014. Quantification of impacts of nitrogen deposition on forest ecosystem services in Europe. Nitrogen deposition, critical Loads and biodiversity, 411-424.

de Vries, W., Reinds, G.J., Vel, E., 2003. Intensive monitoring of forest ecosystems in Europe 2: Atmospheric deposition and its impacts on soil solution chemistry. Forest Ecology and Management 174, 97-115.

De Vries, W., Van der Salm, C., Reinds, G., Erisman, J., 2007. Element fluxes through European forest ecosystems and their relationships with stand and site characteristics. Environ Pollut 148, 501-513.

Decina, S.M., Templer, P.H., Hutyra, L.R., 2018. Atmospheric inputs of nitrogen, carbon, and phosphorus across an urban area: Unaccounted fluxes and canopy influences. Earth's Future 6, 134-148.

Dobermann, A., Pampolino, M., Adviento, M., 1997. Resin capsules for on‐site assessment of soil nutrient supply in lowland rice fields. Soil Sci Soc Am J 61, 1202-1213.

Draaijers, G., Erisman, J., Spranger, T., Wyers, G., 1996. The application of throughfall measurements for atmospheric deposition monitoring. Atmos Environ 30, 3349-3361.

Fang, Y.T., Yoh, M., Koba, K., Zhu, W.X., Takebayashi, Y., Xiao, Y.H., Lei, C.Y., Mo, J.M., Zhang, W., Lu, X.K., 2011. Nitrogen deposition and forest nitrogen cycling along an urban-rural transect in southern China. Global Change Biol 17, 872-885.

Fenn, M., Bytnerowicz, A., Schilling, S., Ross, C., 2015. Atmospheric deposition of nitrogen, sulfur and base cations in jack pine stands in the Athabasca Oil Sands Region, Alberta, Canada. Environ Pollut 196, 497-510.

Fenn, M.E., Bytnerowicz, A., Schilling, S.L., 2018. Passive monitoring techniques for evaluating atmospheric ozone and nitrogen exposure and deposition to California ecosystems. Gen. Tech. Rep. PSW-GTR-257. Albany, CA: US Department of Agriculture, Forest Service, Pacific Southwest Research Station 257.

Fenn, M.E., Poth, M.A., 2004. Monitoring nitrogen deposition in throughfall using ion exchange resin columns: A field test in the San Bernardino Mountains. J Environ Qual 33, 2007-2014.

Fenn, M.E., Poth, M.A., Arbaugh, M.J., 2002. A throughfall collection method using mixed bed ion exchange resin columns. TheScientificWorldJOURNAL 2, 122-130.

Garcia-Gomez, H., Izquieta-Rojano, S., Aguillaume, L., Gonzalez-Fernandez, I., Valino, F., Elustondo, D., Santamaria, J.M., Avila, A., Fenn, M.E., Alonso, R., 2016. Atmospheric deposition of inorganic nitrogen in Spanish forests of Quercus ilex measured with ion-exchange resins and conventional collectors. Environ Pollut 216, 653-661.

Hart, S., Binkley, D., 1984. Colorimetric interference and recovery of adsorbed ions from ion exchange resins. Communications in Soil Science and Plant Analysis 15, 893-902.

Hislop, J.E., Hornbeck, J.W., 2002. Coping with effects of high dissolved salt samples on the inductively coupled plasma spectrometer. Communications in soil science and plant analysis 33, 3377-3388.

Hoffman, A.S., Albeke, S.E., McMurray, J.A., Evans, R.D., Williams, D.G., 2019. Nitrogen deposition sources and patterns in the Greater Yellowstone Ecosystem determined from ion exchange resin collectors, lichens, and isotopes. Sci Total Environ 683, 709-718.

Horswill, P., O'Sullivan, O., Phoenix, G.K., Lee, J.A., Leake, J.R., 2008. Base cation depletion, eutrophication and acidification of species-rich grasslands in response to long-term simulated nitrogen deposition. Environ Pollut 155, 336-349.

585   Houdijk, A., Verbeek, P., Van Dijk, H., Roelofs, J., 1993. Distribution and decline of endangered herbaceous heathland species in relation to the chemical composition of the soil. Plant and Soil 148, 137-143.

Ibrahim, M.H., Metali, F., U Tennakoon, K., Sukri, R.S., 2022. Impacts of invasive Acacias on ion deposition in a coastal Bornean tropical heath forest. Journal of Forest Research 27, 20-27.

Johansson, K., Bergbäck, B., Tyler, G., 2001. Impact of atmospheric long range transport of lead, mercury and cadmium on 590   the Swedish forest environment. Water, Air and Soil Pollution: Focus 1, 279-297.

Kjonaas, O.J., 1999. Factors affecting stability and efficiency of ion exchange resins in studies of soil nitrogen transformation. Communications in soil science and plant analysis 30, 2377-2397.

KNMI, 2022. LH15, langjarige gemiddelden, tijdvak 1991-2020.

Kohler, S., Jungkunst, H.F., Gutzler, C., Herrera, R., Gerold, G., 2012. Atmospheric Ionic Deposition in Tropical Sites of 595   Central Sulawesi Determined by Ion Exchange Resin Collectors and Bulk Water Collector. Water Air Soil Poll 223, 4485-4494.

Krupa, S., Legge, A., 2000. Passive sampling of ambient, gaseous air pollutants: an assessment from an ecological perspective. Environ Pollut 107, 31-45.

Langlois, J.L., Johnson, D.W., Mehuys, G.R., 2003. Adsorption and recovery of dissolved organic phosphorus and nitrogen by mixed‐bed ion‐exchange resin. Soil Sci Soc Am J 67, 889-894.

600   Lovett, G.M., Reiners, W.A., 1986. Canopy structure and cloud water deposition in subalpine coniferous forests. Tellus B: Chemical and Physical Meteorology 38, 319-327.

Lu, X., Mao, Q., Gilliam, F.S., Luo, Y., Mo, J., 2014. Nitrogen deposition contributes to soil acidification in tropical ecosystems. Global Change Biol 20, 3790-3801.

Mamo, M., Ginting, D., Renken, R., Eghball, B., 2004. Stability of ion exchange resin under freeze–thaw or dry–wet 605   environment. Soil Sci Soc Am J 68, 677-681.

Nicholas Clarke, D.Z., Erwin Ulrich, Rosario Mosello, John Derome, Kirsti Derome, Nils, König, G.L., Geert P.J. Draaijers, Karin Hansen, Anne Thimonier, Peter Waldner, 2016. Manual on methods and criteria for harmonized sampling, assessment, monitoring and analysis of the effects of air pollution on forests. Part XIV Sampling and Analysis of Deposition.

Park, S.-C., Cho, H.-R., Lee, J.-H., Yang, H.-Y., YANG, O.-B., 2014. A study on adsorption and desorption behaviors of 14C 610   from a mixed bed resin. Nuclear Engineering and Technology 46, 847-856.

Pey, J., Larrasoaña, J.C., Pérez, N., Cerro, J.C., Castillo, S., Tobar, M.L., de Vergara, A., Vázquez, I., Reyes, J., Mata, M.P., 2020. Phenomenology and geographical gradients of atmospheric deposition in southwestern Europe: Results from a multi-site monitoring network. Sci Total Environ 744, 140745.

Qian, P., Schoenau, J., 2002. Practical applications of ion exchange resins in agricultural and environmental soil research. 615   Canadian Journal of soil science 82, 9-21.

Rabalais, N.N., 2002. Nitrogen in aquatic ecosystems. AMBIO: a Journal of the Human Environment 31, 102-112.

Risch, A.C., Zimmermann, S., Moser, B., Schütz, M., Hagedorn, F., Firn, J., Fay, P.A., Adler, P.B., Biederman, L.A., Blair, J.M., 2020. Global impacts of fertilization and herbivore removal on soil net nitrogen mineralization are modulated by local climate and soil properties. Global Change Biol 26, 7173-7185.

620   RIVM, 2015. LMRe Regenwaterstamenstelling 2015.

Sheibley, R.W., Foreman, J.R., Moran, P.W., Swarzenski, P.W., 2012. Atmospheric deposition, water-quality, and sediment data for selected lakes in Mount Rainier, North Cascades, and Olympic National Parks, Washington, 2008–2010. US Geological Survey Data Series 721, 34.

Sheng, W., Yu, G., Jiang, C., Yan, J., Liu, Y., Wang, S., Wang, B., Zhang, J., Wang, C., Zhou, M., 2013. Monitoring nitrogen 625   deposition in typical forest ecosystems along a large transect in China. Environmental monitoring and assessment 185, 833-844.

Simkin, S.M., Lewis, D.N., Weathers, K.C., Lovett, G.M., Schwarz, K., 2004. Determination of sulfate, nitrate, and chloride in throughfall using ion-exchange resins, Water Air Soil Poll, pp. 343-354.

Skogley, E.O., Dobermann, A., 1996. Synthetic ion‐exchange resins: Soil and environmental studies. J Environ Qual 25, 13-630   24.

Solberg, S., Dobbertin, M., Reinds, G.J., Lange, H., Andreassen, K., Fernandez, P.G., Hildingsson, A., de Vries, W., 2009. Analyses of the impact of changes in atmospheric deposition and climate on forest growth in European monitoring plots: a stand growth approach. Forest Ecology and Management 258, 1735-1750.

Staelens, J., Houle, D., De Schrijver, A., Neirynck, J., Verheyen, K., 2008. Calculating dry deposition and canopy exchange 635   with the canopy budget model: review of assumptions and application to two deciduous forests. Water, Air, and Soil Pollution 191, 149-169.

Stevens, C.J., Dise, N.B., Mountford, J.O., Gowing, D.J., 2004. Impact of nitrogen deposition on the species richness of grasslands. Science 303, 1876-1879.

Szillery, J.E., Fernandez, I.J., Norton, S.A., Rustad, L.E., White, A.S., 2006. Using ion-exchange resins to study soil response 640   to experimental watershed acidification. Environmental monitoring and assessment 116, 383-398.

Tahovská, K., Čapek, P., Šantrůčková, H., Kaňa, J., Kopáček, J., 2016. Measurement of in situ phosphorus availability in acidified soils using iron-infused resin. Communications in Soil Science and Plant Analysis 47, 487-494.

Thimonier, A., 1998. Measurement of atmospheric deposition under forest canopies: some recommendations for equipment and sampling design. Environmental Monitoring and Assessment 52, 353-387.

645   Tulloss, E.M., Cadenasso, M.L., 2015. Nitrogen deposition across scales: Hotspots and gradients in a California savanna landscape. Ecosphere 6, 1-12.

Van Dam, D., Heil, G., Heijne, B., 1987. Throughfall chemistry of grassland vegetation: A new method with ion-exchange resins. Functional Ecology, 423-427.

Van Dam, D., Heil, G., Heijne, B., Bobbink, R., 1991. Throughfall below grassland canopies: a comparison of conventional
650   and ion exchange methods. Environ Pollut 73, 85-99.

Van Langenhove, L., Verryckt, L.T., Bréchet, L., Courtois, E.A., Stahl, C., Hofhansl, F., Bauters, M., Sardans, J., Boeckx, P., Fransen, E., 2020. Atmospheric deposition of elements and its relevance for nutrient budgets of tropical forests. Biogeochemistry 149, 175-193.

Vos, M.A., den Ouden, J., Hoosbeek, M., Valtera, M., de Vries, W., Sterck, F., 2023a. The sustainability of timber and biomass
655   harvest in perspective of forest nutrient uptake and nutrient stocks. Forest Ecology and Management 530, 120791.

Vos, M.A.E., de Boer, D., de Vries, W., den Ouden, J., Sterck, F.J., 2023b. Aboveground carbon and nutrient distributions are hardly associated with canopy position for trees in temperate forests on poor and acidified sandy soils. Forest Ecology and Management 529, 120731.

Wieder, R.K., Vile, M.A., Albright, C.M., Scott, K.D., Vitt, D.H., Quinn, J.C., Burke-Scoll, M., 2016. Effects of altered
660   atmospheric nutrient deposition from Alberta oil sands development on Sphagnum fuscum growth and C, N and S accumulation in peat. Biogeochemistry 129, 1-19.

Xu, W., Zhang, L., Liu, X., 2019. A database of atmospheric nitrogen concentration and deposition from the nationwide monitoring network in China. Scientific data 6, 1-6.

Yamashita, N., Sase, H., Kobayashi, R., Leong, K.-P., Hanapi, J.M., Uchiyama, S., Urban, S., Toh, Y.Y., Muhamad, M.,
665   Gidiman, J., 2014. Atmospheric deposition versus rock weathering in the control of streamwater chemistry in a tropical rain-forest catchment in Malaysian Borneo. Journal of tropical ecology 30, 481-492.

Zarrabi, M., Soori, M.M., Sepehr, M.N., Amrane, A., Borji, S., Ghaffari, H.R., 2014. Removal of phosphorus by ion-exchange resins: equilibrium, kinetic and thermodynamic studies. Environmental Engineering & Management Journal (EEMJ) 13.

Zuur, A., Ieno, E.N., Walker, N., Saveliev, A.A., Smith, G.M., 2009. Mixed effects models and extensions in ecology with R.
670   Springer Science & Business Media.